

Optimization of 50G-PON APD-based receivers

Original

Optimization of 50G-PON APD-based receivers / Minelli, L., Abdellatif, A., Gaudino, R.. - ELETTRONICO. - (2022), pp. 1-4. (2022 Italian Conference on Optics and Photonics (ICOP) Trento, Italy 15-17 June 2022) [10.1109/ICOP56156.2022.9911721].

Availability:

This version is available at: 11583/2972472 since: 2022-10-21T11:29:47Z

Publisher:

IEEE

Published

DOI:10.1109/ICOP56156.2022.9911721

Terms of use:

This article is made available under terms and conditions as specified in the corresponding bibliographic description in the repository

Publisher copyright

IEEE postprint/Author's Accepted Manuscript

©2022 IEEE. Personal use of this material is permitted. Permission from IEEE must be obtained for all other uses, in any current or future media, including reprinting/republishing this material for advertising or promotional purposes, creating new collecting works, for resale or lists, or reuse of any copyrighted component of this work in other works.

(Article begins on next page)

Optimization of 50G-PON APD-based receivers

Leonardo Minelli
Politecnico di Torino (DET)
 Torino, Italy
 leonardo.minelli@polito.it

Ahmed Abdellatif
Politecnico di Torino (DET)
 Turin, Italy

Roberto Gaudino
Politecnico di Torino (DET)
 Turin, Italy

Abstract—In this paper, we approach the optimization of IM-DD systems leveraging APD-based receivers and Feed-Forward Equalization (FFE) at the receiver side (RX). We review the role of APD-based receivers in recent evolutions of IEEE and ITU-T standards for high-speed Passive Optical Networks (PON) and in particular in 50G-PON as discussed in the recently approved Recommendation ITU-T G.9804.3. We analyze different optimization methods for PAM-2 (NRZ) and PAM-4 modulation formats, based on grid search methods and analytical closed-form solutions for decision thresholds and PAM-4 internal levels. We develop our study on a simulated optical IM-DD system, transmitting at a Baud Rate $R_s=50$ GBaud (i.e., 50 Gbps for NRZ, 100 Gbps for PAM-4). We assess power budget gain in terms of Optical Path Loss (OPL) with respect to nominal thresholds and levels, determining that optimizations are effective (i.e., approximately 1 dB OPL gain) when the system has moderate bandwidth limitations ($B_{3dB} > 0.5 \cdot R_s$). Our study can be of interest in the future for a better definition of the TDEC parameter for APD-based receivers.

Index Terms—IM-DD systems, APD-based Receivers, 50G-Passive Optical Networks

I. INTRODUCTION

Passive Optical Networks (PON) are today by far the most commonly used optical access network architecture, with commercial deployments of the order of 100 million Optical Network Units (ONU) per year worldwide, mostly in the GPON and XG-PON versions. ITU-T and IEEE are currently standardizing the PON next generation at 50 Gbps/s/ λ and above. In particular, ITU-T has very recently standardized in [1] downstream transmission at 50Gbit/s using traditional PAM-2 OOK direct-detection. For the first time anyway, this PON standard has introduced receiver feed-forward equalization (FFE) and avalanche-photodiode APD-based receivers (APD-RX), and also a variant of the Transmitter and Dispersion Eye Closure (TDEC) parameter to assess transmitter performance that includes both features (i.e. that takes into account APD noise and FFE).

In this paper, we thus investigate APD-RX optimization, analyzing APD-RX noise, which tends to be asymmetric on the received PAM-M levels, being instantaneously proportional to the useful signal optical power, a feature that was already discussed in some previous papers, such as [2] and [3] but that tends to be neglected in most other papers focused on PAM-4 but for short-reach data center applications (such as [4], [5] and [6]). We investigated in particular both PAM-2 at 50 Gbit/s and PAM-4 at 100 Gbit/s, optimizing the APD-RX decision thresholds inside a DSP-based FFE and, for PAM-4 only, the

optimization of the two internal PAM-4 transmitted levels, focusing on minimization of BER parameter and assessing the related system gain in term of increased Optical Path Loss (OPL) at a given target BER. Our work can in the near future be applied to a better definition of the TDEC parameter in the specific framework of high-speed PON, such as in [1].

II. NOISE IN APD-BASED RECEIVERS

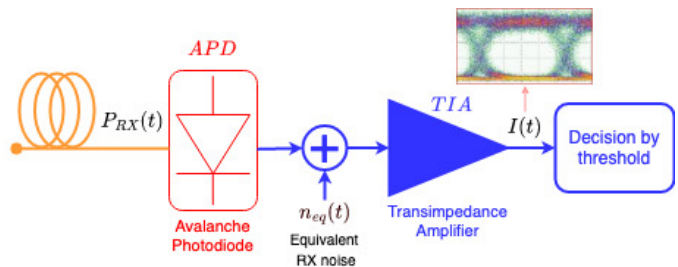


Fig. 1. Schematics of an ADP-based Receiver

APD-based receivers (illustrated in Fig. 1) have been considered in 50G-PON (as well as in previous XGS-PON), due to the better sensitivity provided by the Avalanche photodiodes with respect to the more commonly adopted PIN photodetectors. However, APD-based receivers are affected by signal-dependent Gaussian noise components. By jointly considering the effect of the TIA thermal noise and APD shot noise, the equivalent APD-based RX noise $n_{eq}(t)$ can be then modeled as a WGN with signal-dependent (and thus time-dependent) variance:

$$\sigma_{eq}^2(t) = \sigma_{th}^2 + \sigma_{shot}^2(t) \quad (1)$$

where $\sigma_{th}^2 = IRND^2 \cdot B$ is the TIA thermal noise time-independent variance (being $IRND$ the input referred noise density), and $\sigma_{shot}^2(t)$ is the time-dependent variance of the APD shot noise, defined as:

$$\sigma_{shot}^2(t) = 2qFG^2RB \cdot P_{RX}(t) \quad (2)$$

where q is the electron charge, F is the excess noise figure, G and R are respectively the APD gain and responsivity, B is the noise bandwidth and $P_{RX}(t)$ is the instantaneous RX power.

As a result, the RX signal current $I(t)$ is affected by an unbalanced disturbance, since the APD noise variance increases proportionally to the instantaneous optical power. An example is provided in the NRZ eye-diagram in Fig. 1.

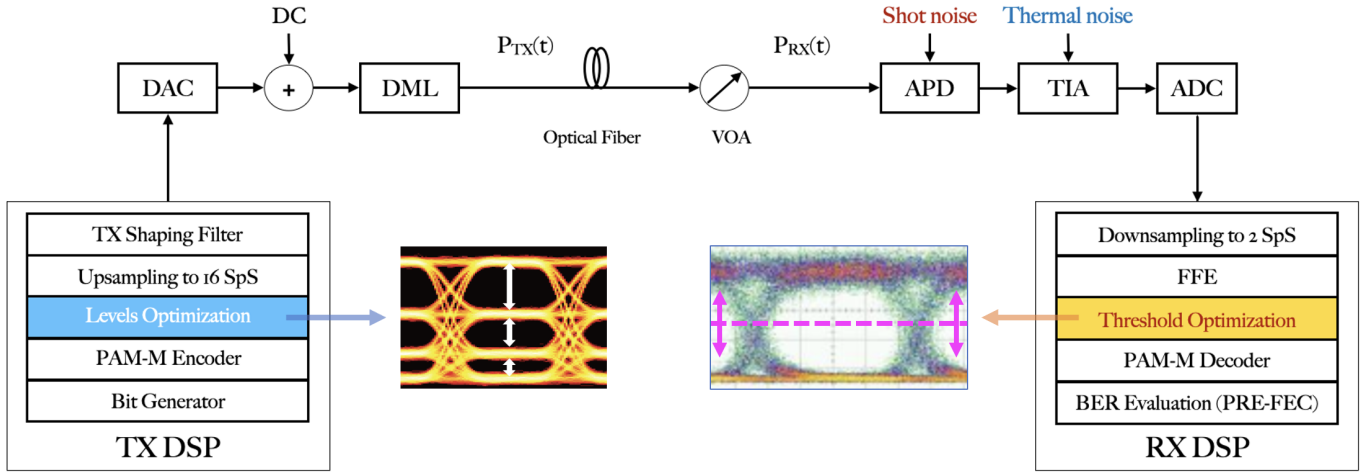


Fig. 2. Schematics of the simulated optical transmission system. Inset figures: (left) PAM-4 internal levels optimization; (right) PAM-2 decision threshold optimization.

III. SIMULATION SETUP

A schematics of the simulated transmission system that we used in this paper is illustrated in Fig. 2. Simulations were conducted by transmitting a pseudo-random binary sequence (PRBS), encoded into PAM-2 or PAM-4 modulation format, with a Baud Rate $R_s = 50$ GBaud (i.e., corresponding to 50 Gbit/s for PAM-2 and 100 Gbit/s for PAM-4). After shaping the symbols with a Bessel filter (order 4, B_{3dB} equal to 70% of the Baud Rate), the signal was injected into an optical channel through a linear Direct Modulated Laser (DML) ($\bar{P}_{TX} = 0$ dBm). The use of an ideal Digital-to-Analog Converter (DAC) has been assumed. The analog channel has been simulated by upsampling the signal to a 16 sample-per-symbol (sps) ratio. We performed a Back-to-Back (B2B) analysis, neglecting linear and nonlinear optical fiber effects. To then assess different values of Optical Path Loss (OPL), a Variable Optical Attenuator (VOA) was applied to the waveform. The optical signal was thus converted into the electrical domain through an APD and then amplified using a TIA. APD shot and TIA thermal noise have been characterized under realistic assumptions, by taking as reference the parameters adopted in [7]: a brief summary is reported in Table I.

TABLE I
RX NOISE PARAMETERS

APD Responsivity R	0.7 A/W
APD Gain G	10 dB
APD Excess noise figure F	7.1 dB
TIA Input-Referred Noise Density $IRND$	15 pA/ \sqrt{Hz}

At the RX side, after resampling to 2 sps (under ideal ADC assumption), we applied a fractionally spaced FFE with 31 taps, to then decode the bits through threshold-based hard decision and evaluate the pre-FEC BER.

IV. THRESHOLDS AND LEVELS OPTIMIZATION

In this paper, we investigated optimization options for improving the performance of IM-DD systems with APD-based receivers. First, we searched for the optimal decision thresholds at RX for PAM-2 and PAM-4 modulation formats. We then approached the optimization at the TX side of the internal levels in the PAM-4 modulation format (see Figure 2, left eye-diagram).

A. RX Thresholds Optimization

Threshold optimization was performed by following two different approaches. The first one we studied was based on an exhaustive search for threshold values, by systematically evaluating the system BER using different values for the decision thresholds, and then selecting the ones leading to the best performance. In the second approach instead, we relied on a closed-form calculation of the threshold values. We verified indeed that, with a small approximation, the probability density functions (p.d.f.) of the equalized RX symbols, conditioned on the TX PAM- M level, correspond to M different Gaussian distributions, as follows:

$$f(y|x = a_i) = \frac{1}{\sigma_i \sqrt{2\pi}} e^{-\frac{1}{2} \left(\frac{y - \mu_i}{\sigma_i} \right)^2} \quad i = 1, \dots, M \quad (3)$$

where $f(y|x = a_i)$ is the p.d.f. of the equalized RX symbol y when the TX symbol x is $a_i \in [a_1, \dots, a_M]$.

This assumption allows to analytically compute the optimal thresholds, after estimating the centroids μ_i and the variances σ_i^2 of the RX symbols after the FFE. By considering for instance the PAM-2 case ($M = 2$, $a_1 < a_2$), the optimal threshold can be analytically computed by minimizing the error probability, defined as:

$$P(e) = \frac{1}{2} P(y > T_h | x = a_1) + \frac{1}{2} P(y < T_h | x = a_2) \quad (4)$$

where T_h is the decision threshold. The optimal value of T_h can be optimized by nullifying the derivative of $P(e)$ with respect to the threshold, leading to the following equality:

$$f(y = T_h|x = a_1) = f(y = T_h|x = a_2) \quad (5)$$

By substituting Eq.3 in Eq.5, a second order equation with respect to T_h can be obtained, which leads to the solution below (assuming $a_1 < a_2$):

$$T_h^* = \frac{-b + \sqrt{b^2 - 4ac}}{2a} \quad (6)$$

$$a = \frac{1}{2\sigma_1^2} - \frac{1}{2\sigma_2^2}$$

$$b = \frac{\mu_2}{\sigma_2^2} - \frac{\mu_1}{\sigma_1^2}$$

$$c = \frac{\mu_1^2}{2\sigma_1^2} - \frac{\mu_2^2}{2\sigma_2^2} - \ln\left(\frac{\sigma_2}{\sigma_1}\right)$$

where T_h^* is the optimal threshold value. This derivation can be easily extended to any PAM-M modulation, by solving Eq.5 for each pair of adjacent levels a_i and a_{i+1} ($i = 1, \dots, M-1$). Moreover, if the variances do not assume too different values, a further approximation for optimal threshold computation can be the Equation 18 proposed in [3].

In this case study, the second approach resulted to provide thresholds approximately equal to those obtained through iterative search, with the advantage of being significantly faster thanks to the closed-form computation.

B. TX Levels Optimization

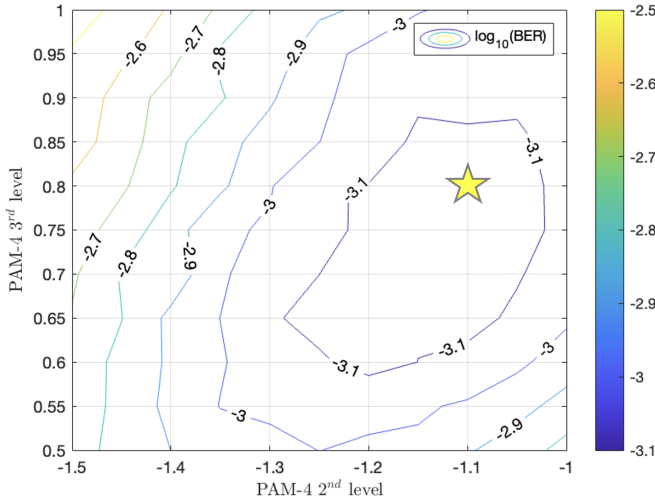


Fig. 3. BER contour plot related to PAM-4 inner TX levels optimization (nominal values: -3,-1,+1,+3), simulating the system with OPL=20 dB and ER=11 dB. Horizontal axis: tested values for the 2nd level (nominally equal to -1). Vertical axis: tested values for the 3rd level (nominally equal to +1). The yellow star indicates the optimal inner levels combination.

Concerning the PAM-4 modulation format, we investigated the optimization of the internal levels at the TX side (i.e., the 2nd and the 3rd ones), while fixing the outer Optical Modulation Amplitude (OMA). Differently from RX thresholds, we could not rely on closed-form solutions for optimal

values: therefore we followed a grid search approach [8]: we evaluated the BER over a manually specified subset of the inner levels search space, looking for the combination giving the best performance. An example of grid-search-based TX level optimization (i.e., with OPL=20 dB, ER=11 dB) in our study is illustrated in Fig. 3.

V. SIMULATION RESULTS

By applying the optimizations illustrated in Section IV, we evaluated the BER performance in the considered simulation scenario, testing the transmission system in different conditions using PAM-2 and PAM-4 modulation formats. During simulation, we use direct BER counting on a string of $2 \cdot 10^5$ transmitted bits.

In Fig. 4 the simulation results are illustrated in terms OPL vs Extinction Ratio (ER) curves, for BER target equal to 10^{-2} and 10^{-3} . We compared the performance when no optimization is applied (i.e. symmetric thresholds, equally spaced TX levels) with respect to the case in which RX thresholds and/or TX levels are optimized. As it can be observed, APD-based receivers benefit from optimizing the decision thresholds when transmitting NRZ signals, with a gain of approximately 0.6 dB in terms of OPL for every considered ER (BER= 10^{-3}). Threshold optimization alone is instead less effective when PAM-4 sequences are transmitted: the reason is that the thresholds in this situation can't be modified as much as in the PAM-2 case (i.e., they are constrained between closer levels). Optimizing also the transmitted internal PAM-4 levels leads anyway to an effective gain, that reaches up to 1 dB in terms of OPL for higher ER (BER= 10^{-3}).

To assess the effectiveness of the optimizations as a function of the bandwidth limitations in the transmission system, we evaluated the system performance in terms of OPL versus 3-dB Bandwidth. The related results for BER= 10^{-2} and BER= 10^{-3} are illustrated in Fig. 5. As it can be noticed, the optimization of both decision thresholds and TX levels exhibits a decreasing performance gain as the bandwidth is lower. As indeed the Inter Symbol Interference (ISI) gets higher due to bandwidth limitations, the FFE needs to correlate an increasing number of pre- and post- cursors to equalize the RX sequence. The level-dependent effect of the RX noise gets thus averaged over the several combined symbols, leading to a disturbance that after equalization is no longer asymmetric: therefore, the optimizations become useless (i.e., the optimal values for thresholds and levels converge to the nominal ones).

VI. CONCLUSION AND DISCUSSION

In this paper, we studied the optimization of IM-DD systems leveraging APD-based receivers. We optimized the decision thresholds for symbols after FFE and the inner PAM-4 inner levels for fixed outer OMA. The work presented in this paper is of interest for the 50G-PON ITU-T standard using NRZ at 50 Gbps, due to the very likely adoption in these networks of APD receivers and FFE equalization at the RX side. Moreover, the analyzed TX level optimization can be useful toward the adoption in the next-generation PON of PAM-4 at 100 Gbps.

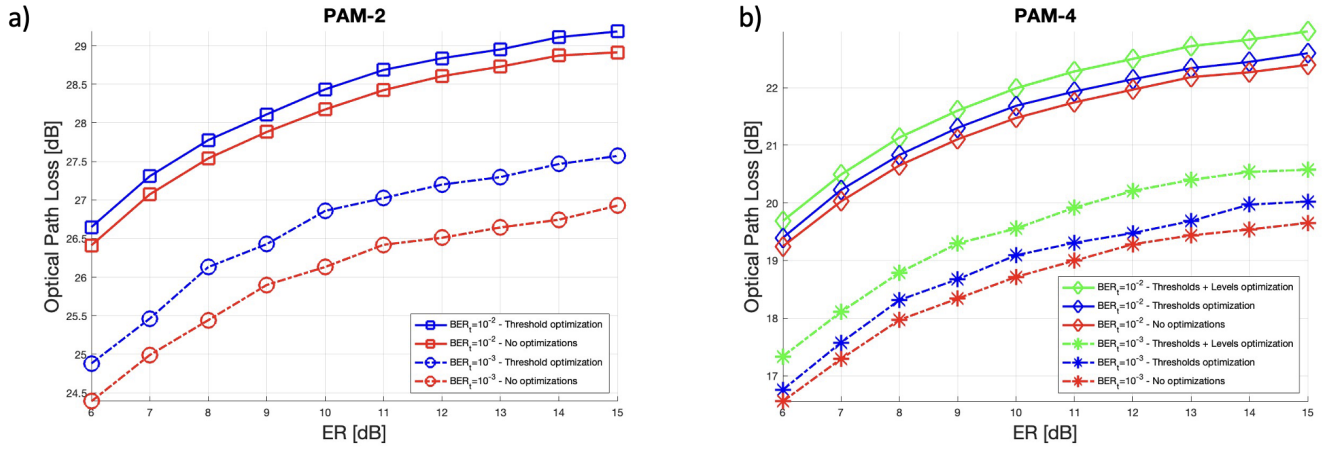


Fig. 4. Optical Path Loss (OPL) versus Extinction Ratio (ER) performance comparison with and without optimizations a) using PAM-2 (NRZ) modulation format b) using PAM-4 modulation format.

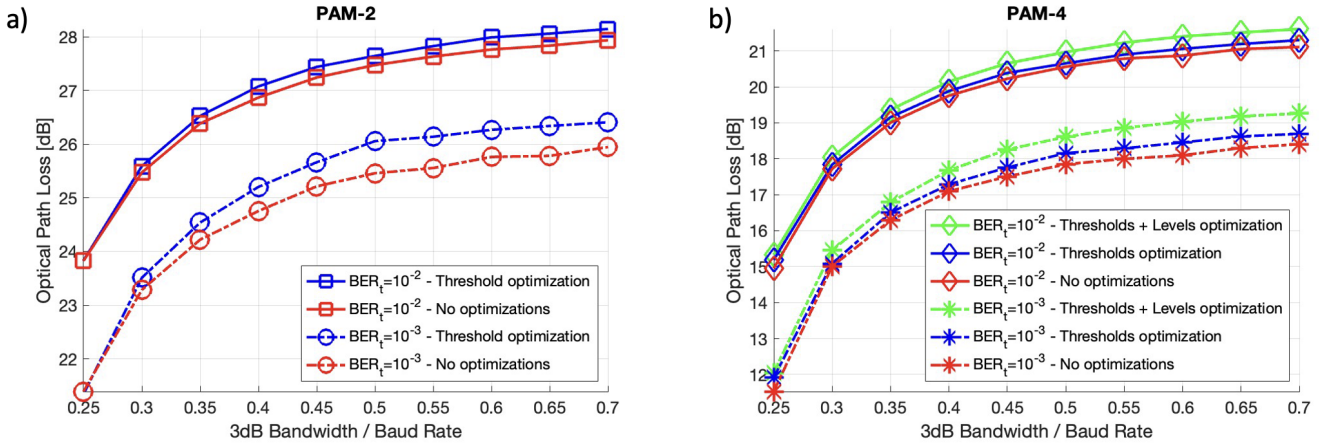


Fig. 5. Optical Path Loss (OPL) versus system's 3-dB bandwidth performance comparison with and without optimizations a) using PAM-2 (NRZ) modulation format b) using PAM-4 modulation format.

ACKNOWLEDGMENT

We acknowledge the PhotoNext initiative at Politecnico di Torino (<http://www.photonext.polito.it/>)

REFERENCES

- [1] ITU-T G.9804 Series of Recs., "50-Gigabit-capable passive optical networks (50G-PON): Physical media dependent (PMD) layer specification," G.9804.3 (50G-PON PMD), Approved in 2021-09-06.
- [2] G. Katz and E. Sonkin, "Level Optimization of PAM-4 Transmission With Signal-Dependent Noise," *IEEE Photonics Journal*, vol. 11, no. 1, pp. 1–6, 2019.
- [3] K. Ho and J. M. Kahn, "Multilevel optical signals optimized for systems having signal-dependent and signal-independent noises, finite transmitter extinction ratio and intersymbol interference," Feb. 10 2004, uS Patent 6,690,894.
- [4] D. Sadot, G. Dorman, A. Gorshtein, E. Sonkin, and O. Vidal, "Single channel 112Gbit/sec PAM4 at 56Gbaud with digital signal processing for data centers applications," *Optics express*, vol. 23, no. 2, pp. 991–997, 2015.
- [5] A. Dochhan, H. Griesser, N. Eiselt, M. H. Eiselt, and J.-P. Elbers, "Solutions for 80 km DWDM Systems," *Journal of Lightwave Technology*, vol. 34, no. 2, pp. 491–499, 2016.
- [6] N. Eiselt, J. Wei, H. Griesser, A. Dochhan, M. Eiselt, J.-P. Elbers, J. J. V. Olmos, and I. T. Monroy, "First real-time 400G PAM-4 demonstration for inter-data center transmission over 100 km of SSMF at 1550 nm," in *Optical Fiber Communication Conference*. Optica Publishing Group, 2016, pp. W1K–5.
- [7] P. Torres-Ferrera, H. Wang, V. Ferrero, and R. Gaudino, "100 Gbps/λ PON downstream O- and C-band alternatives using direct-detection and linear-impairment equalization [Invited]," *Journal of Optical Communications and Networking*, vol. 13, no. 2, pp. A111–A123, 2021.
- [8] I. J. Goodfellow, Y. Bengio, and A. Courville, *Deep Learning*. Cambridge, MA, USA: MIT Press, 2016, <http://www.deeplearningbook.org>.